

Additional File 1 Figure Legends

Additional File 1: Fig. S1. Quality control of HA-CTCF ChIP-seq in the presence of RNA-binding deficiency or RNA depletion.

(A) Schematic diagram illustrating how the ectopic HA-tagged CTCF swap system works in combination with acute protein degradation of endogenous CTCF. The homozygous miniAID-mClover3 knockin SEM cell line, CTCF^{AID2}, was generated in our previous study [11]. The 5-Ph-IAA auxin analog is added to cell culture for 6 hours, binds to the miniAID tag (fused to endogenous CTCF protein) and recruits binding to the OsTIR1(F74G) protein and the SCF complex, which ubiquitinates the CTCF protein leading to acute degradation. Concurrently, the CTCF HA-tagged WT or RNA-binding region deficient form is induced by doxycycline for an additional 18 hours.

(B) Immunoblot analysis of endogenous (CTCF^{AID2.0}) and induced exogenous (HA-CTCF) expression of CTCF using an antibody for CTCF. CTCF^{AID2.0} expression can be seen in all untreated samples (-, -). After 6 hours of 10 μ M 5-Ph-IAA treatment, CTCF^{AID2} protein expression is degraded. Exogenous expression of HA-tagged CTCF wildtype and dRBR mutant is comparable to endogenous CTCF following 18 hours of 1 μ g/mL doxycycline with concurrent 10 μ M 5-Ph-IAA treatment (+, +). GAPDH was included as a loading control. The dZF1 and dZF10 mutant forms of CTCF were included as positive blotting controls to indicate the accurate molecular weight.

(C) Reproducible HA ChIP-seq signals were used from CTCF^{AID2/WT} cells and CTCF^{AID2/dRBR} cells, Triptolide, RNase A, and DMSO treatment groups to conduct the Spearman's correlation, which was calculated to quantify the overall similarity between samples.

(D) Violin plot of the peak score of ChIP-seq from CTCF-antibody only peaks and shared peaks between HA and CTCF-antibody pulldown.

Additional File 1: Fig. S2. Quality control of Triptolide and RNase A treatment conditions for CTCF ChIP-seq.

(A) Q-PCR was conducted to quantify the transcription decrease of *MYC*, *RBM45*, and *CTCF* in response to Triptolide treatment (4 hours) in a dosage-dependent manner.

(B) Q-PCR was conducted to quantify the transcription decrease of *MYC*, *RBM45*, and *CTCF* in response to Triptolide treatment (0.1 and 1 μ M) in a time-course manner.

(C) Dead cell % quantification was conducted in cells in response to Triptolide treatment (0.1 and 1 μ M) in a time-course manner.

(D) Q-PCR was conducted to quantify the transcription decrease of *MYC* (short half-life) and *GAPDH* (long half-life) in response to RNase A treatment (1mg/mL) in a time-course manner.

(E) In the pre-fixation RNase A treatment group, a pilot fraction of samples was collected for Q-PCR against *MYC*, *RBM45*, *CTCF*, and *GAPDH* to confirm the RNA depletion efficiency.

(F) Replicate ChIP-seq samples were tested for immunoprecipitation efficiency by CTCF-antibody mediated pull-down and immunoblotting against CTCF in each RNase A treatment and control group. I: Input; FT: flow-through fraction; E: elution fraction.

(G) Replicate ChIP-seq samples were tested for immunoprecipitation efficiency by CTCF-antibody mediated pull-down and immunoblotting against CTCF in each Triptolide treatment and DMSO group. I: Input; FT: flow-through fraction; E: elution fraction.

Additional File 1: Fig. S3. CTCF ChIP-seq analysis for CTCF-RNA interaction interference.

(A) Reproducible CTCF ChIP-seq signals were used from Triptolide and DMSO treatment groups to conduct Spearman's correlation, which was calculated to quantify the overall similarity between samples.

(B) Reproducible CTCF ChIP-seq signals were used from + RNase A and no treatment groups to conduct Spearman's correlation, which was calculated to quantify the overall similarity between samples.

(C) Genomic heatmap of total reproducible genome-wide CTCF-binding peak signals centered at peak midpoint from Triptolide and DMSO treatment groups (69,222).

(D) Genomic heatmap of total reproducible genome-wide CTCF-binding peak signals centered at peak midpoint from RNase A and no treatment groups (38,728).

Additional File 1: Fig. S4. CTCF's RNA binding region deficiency or global RNA depletion plays a limited role in genome-wide chromatin accessibility and transcription.

(A) Genomic heatmap of genome-wide ATAC-seq signals centered at reproducible ATAC-seq peak midpoints from CTCF^{AID2/WT} cells and CTCF^{AID2/dRBR} cells (137,540). ATAC-seq tracks from CTCF^{AID2} with or without auxin treatment were shown as controls.

(B) Spearman's correlation of all ATAC-seq signals defined by (A) was calculated to quantify the similarity between samples.

(C) Chart comparing differential ATAC-seq peaks between dRBR vs WT at different cutoff stringencies.

(D) Total RNA-seq was performed to quantify the global gene expression changes between CTCF-WT and CTCF-dRBR groups. Differential expression genes were presented based on different cutoff stringencies. N=2.

(E) Total RNA-seq was performed to quantify the global gene expression changes between CTCF-dRBR and CTCF-WT groups based on the cutoff of FDR<0.05. N=2.

(F) Total RNA-seq was performed to quantify the global gene expression changes between CTCF-WT and CTCF-dRBR groups. Differential expression genes were presented based on different cutoff stringencies. N=3.

Fig. S1

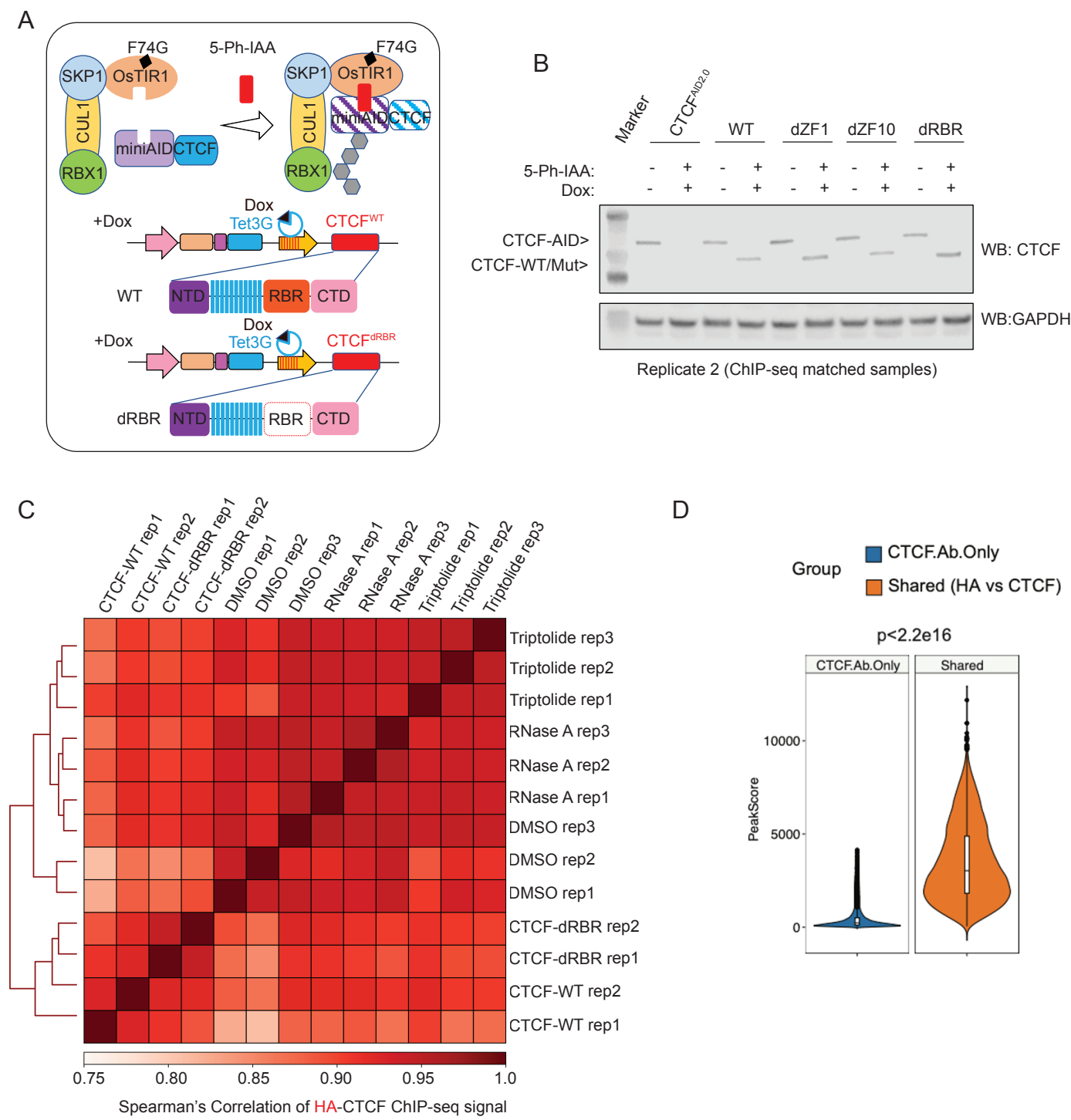


Fig. S2

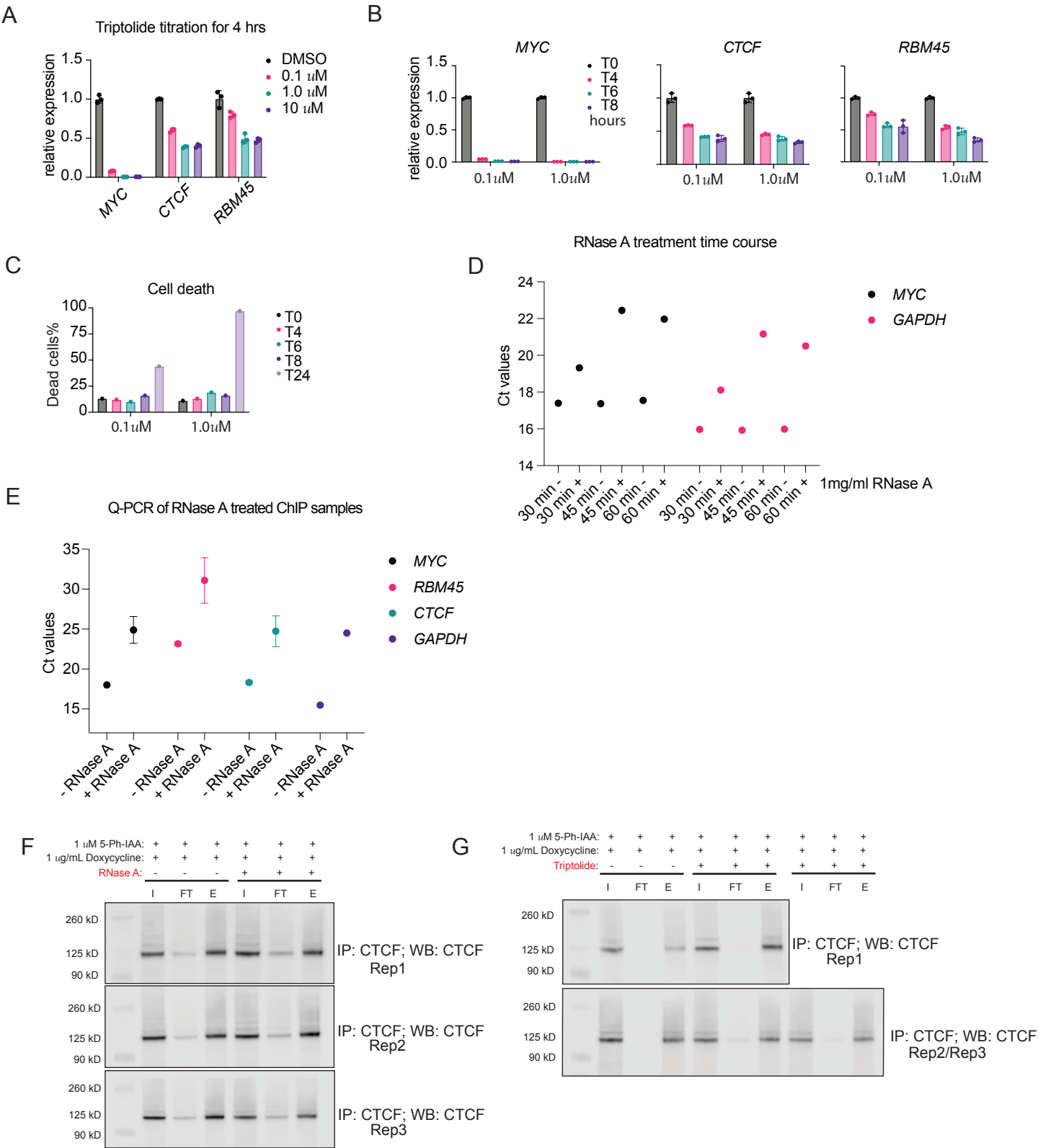


Fig. S3

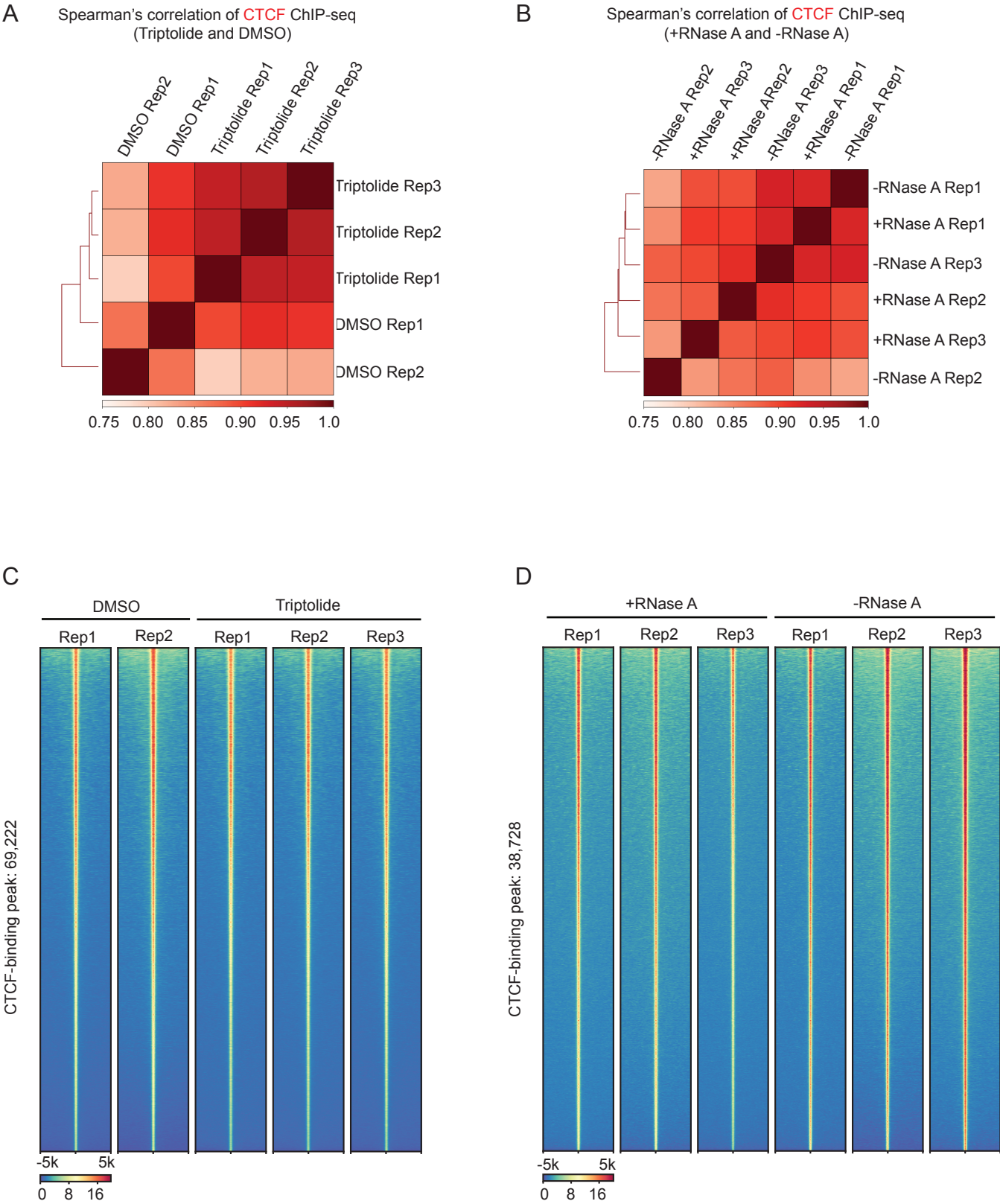


Fig. S4

